New Folder Name Violin Resonance

An Investigation of Violin Resonances in the Test Mass Suspensions of the 40–Meter Mark I Prototype

A. Gillespie and F. Raab
October 5, 1992

Abstract

The mechanical quality factors, or Q's, of the violin resonances of each of the test masses in the 40–meter Mark I Prototype were measured. From the Q's the thermal noise due to the violin modes was estimated. The calculated noise was found to be in agreement with the measured noise of the 40–m prototype near the resonant frequencies of the violin modes.

Introduction

Thermal noise is a fundamental noise source in a gravitational wave detector. Associated with each mode of a physical system in equilibrium with a thermal reservoir is $\frac{1}{2}k_BT$ of thermal energy, where k_B and T are Boltzman's constant and the temperature of the reservoirs, respectively. In order to minimize the effects of this thermal energy to the noise spectrum, it is desirable to concentrate the energy in a very narrow frequency band around the resonant frequency, that is, to have a large quality factor, Q. These narrow frequency bands can then be filtered out of the gravity wave spectrum with little loss of observing bandwidth.

The suspension wires of a gravitational wave detector have several classes of modes which may be sources of thermal noise. We consider here the double wire loop suspension of the test masses in the 40–meter Mark I Prototype. The first class is pendulum modes. These include a polarization along the axis of the beam tube which will couple directly to the interferometer noise as well as a perpendicular polarization and a torsional mode. The next class of modes is the vertical spring modes, including a common mode vertical motion of the mass, a tilt mode, and a roll mode. The vertical modes do not couple directly to the interferometer, but may become important when the resonant optical mode is misaligned from the optic axis of the mirror. The modes which we will concentrate on here are the violin modes, which have two polarizations per wire, one parallel to the optical axis of the interferometer and one transverse to this axis. These

are also poorly coupled to the interferometer in the sense that there is a large mechanical impedance mismatch between the wires and the test mass, but their resonant frequencies lie in the region of several hundred Hertz, right in the middle of the interferometer's observational bandwidth, which makes them an important source of thermal noise.

Violin Resonances and Thermal Noise

The thermal noise in a coarse bandwidth around the violin resonances is well understood.[1] By examining the violin resonances in finer detail one can probe the specific lineshapes of the resonances and hopefully draw conclusions about the damping mechanism. Typically one of two potential damping models is used. The more traditional one, viscous damping, predicts that the damping force is proportional to velocity. This model works well for mechanical systems damped by external forces, such as in eddy current damping of moving conductors or as in gas damping of a pendulum. Recently, Peter Saulson[2] has proposed that a model called internal damping, where damping is modeled by a complex spring constant and the Q is assumed to be frequency independent, may be more realistic when damping is related to internal forces. The lineshapes for these models for a simple oscillator are as follows:

Viscous Damping

$$\tilde{x}^2(f) = \frac{4\,k_B T}{m} \frac{\omega_n/Q}{\left(\omega_n^2 - \omega^2\right)^2 + \omega^2\omega_n^2/Q^2} = 2\pi\,\tilde{x}^2(w) \qquad (1)$$

Internal Damping

$$\tilde{x}^2(f) = \frac{4\,k_B T}{m} \frac{\omega_n^2/Q}{\omega\left[\left(\omega_n^2 - \omega^2\right)^2 + \omega_n^4/Q^2\right]} = 2\pi\,\tilde{x}^2(w) \qquad (2)$$

Here x, ω_n, ω, and m are the amplitude, angular resonant frequency of the n^{th} mode, angular frequency of motion, and effective mass, respectively. Notice that when ω is near ω_n these two lineshapes are approximately equal. With the 40–m Mark I interferometer, the thermal noise of the violin modes dominated other noise only in a narrow band around the violin resonance frequencies, and therefore we could not directly deduce the thermal noise lineshapes far from resonance from

the noise spectrum of the interferometer. However the viscous damping model predicts that $Q \propto \omega_n$, whereas the internal damping model predicts that Q is frequency independent; by examining the Q's of the harmonics of the violin modes to determine the frequency dependence of the Q's, one can discriminate between the two models.

The Q's of the violin modes also provide an important diagnostic of the pendulum Q at frequencies of hundreds of Hertz. For a given amount of bending of the connection of the wire at each end of the suspension, both the violin mode and the pendulum modes have roughly the same energy. Therefore it is reasonable to assume that if the Q's of both the violin modes and the pendulum are limited by losses in the bending of the wire, then both of their Q's should be similar. Since significantly more stretching of the wires occurs in violin modes than in pendulum modes of comparable amplitude, the violin mode Q could be lower than the pendulum Q if wire stretching losses are large. Thus the Q's of the violin modes are currently our best guess for the Q of the pendulum, perhaps representing a pessimistic guess. Since the pendulum motion couples directly to the interferometer, the noise spectrum could be dominated by thermal noise of the pendulum well off resonance, so an estimate of the pendulum Q is important to determine the broad band fundamental limits of the interferometer. For a complete derivation of the pendulum Q's from the wire Q's, see Appendix I.

Measurement Technique

The Q's of individual test mass wires in the 40–m prototype were measured by driving the wires on resonance, turning off the drive, and measuring the ringdown times by filtering the interferometer output, heterodyning it against a local oscillator with a 1 Hz offset and using the decay of the beat note. For the end masses, which have magnets attached to them, the driving signal was applied to the actuator coils.[3] The vertex masses have no magnets and were driven using the piezos on the control block which, in normal use, electronically damp the pendulum motion.[4]

Results of Measurements on the 40–m Prototype

The frequencies and Q's of the lowest (fundamental) violin modes of the 40–m interferometer are given in Figure 1. The differences in frequencies among the different masses may be explained by differences in the suspensions. The

east end mass uses 150–μm-diameter wire.[5] The south end mass uses 100–μm-diameter wire. Both of the vertex masses use 75–μm—diameter wire. The end masses and the vertex masses also have different types of control blocks.

The Q's of the second harmonics of 5 wires were measured — two wires from the east end mass, two wires from the south end mass including both a high and a low Q wire, and a high Q wire from a vertex mass. In addition two additional higher order harmonics of the vertex mass wire were measured. Every one of these harmonics had Q's which were the same as the corresponding fundamental resonance Q within 20%. This result makes a strong case for using the internal damping noise model; any viscous damping mechanism is of minor consequence, at least over this frequency range.

The line shapes of the east end violin resonances were compared with the thermal noise prediction using the internal damping model:[6]

$$\tilde{x}^2(f) = \frac{2\,k_B T}{m}\,\frac{\omega_n^2/Q}{\omega\left[\left(\omega_n^2-\omega^2\right)^2+\omega_n^4/Q^2\right]}\left(\frac{\omega_p}{\omega_n}\right)^2 \qquad (3)$$

where ω_p is the pendulum frequency according to reference 1. The results of this comparison are shown in Figure 2; note that the interferometer spectrum was taken with the electronic damping off. Electronic noise in the damping circuitry enhances the violin motion above thermal noise when the interferometer is in its normal configuration.[7] Also note that some of the resonances are doublets with a much smaller partner. These secondary peaks are presumably the transverse polarizations of the violin modes which do not couple efficiently to the interferometer output. A finer comparison of theory and experiment is given in Figure 3 where the data points (for the middle resonances in Figure 2) are plotted on a linear scale with their associated error bars. The agreement with the thermal noise calculated using the measured resonant frequencies and Q-factors is quite good. The predicted rms fluctuation of the test mass corresponding to a single violin resonance is about 0.06 fm.

Using the measured Q's and assuming that the pendulum mode has a Q as derived in Appendix I, the total thermal noise of the wire suspensions can be predicted. As pointed out above, this is likely a worst case estimate of thermal noise contributed by the suspension. Figure 4 shows this thermal noise prediction and compares it to the measured interferometer noise.

By changing the wire parameters (e.g. density, Q) of these test mass suspensions we can lower the predicted thermal noise at any given frequency (at the expense of other frequencies). There is, however, a noise floor given by mechanical noise leakage through the vibration isolation and suspension systems. Assuming this noise floor is a smooth function of frequency above the first observed violin resonance (at $\sim$300 Hz) we can set an upper limit on it by requiring that it produce less energy in the observed violin resonances than $k_B T$. This upper limit is also shown in Figure 4.

Conclusion

We have analyzed a model which allows us to accurately predict the thermal noise of the violin modes near resonance, given the resonant frequencies and the Q's of the wires. The next steps go in two directions. One area of research will be to understand what limits the Q's of the violin modes and to develop techniques to reliably suspend masses with the highest Q's possible on every wire as opposed to the order of magnitude variations that currently exist. High Q's on every wire are important not only to minimize the noise at each violin resonance, but also because the lowest Q wires may dominate the pendulum thermal noise. The other area of research will be to understand better the relationship between the pendulum Q and the violin Q's. To do this we need to measure the vertical spring mode Q to get an idea of the intrinsic losses of the wires due to stretching. By comparing this Q to the violin Q's we hope to be able to determine whether violin losses are predominantly due to stretching or bending. Even then there is a danger in comparing Q's at frequencies which are different by an order of magnitude, since other frequency dependent damping mechanisms may become important at different frequencies. Avoiding this difficulty will eventually require a direct measurement of the Q of the pendulum resonance near 1 Hz.

Acknowledgments

We would like to acknowledge P. Saulson, R. Weiss and S. Whitcomb for stimulating conversations and M. Zucker and S. Kawamura for helping set up the measurements.

Appendix I: The Pendulum Q

This Appendix shows the derivation of the pendulum Q from the violin Q's assuming that the losses are concentrated in the bending of the wire near its endpoints. These "bending" losses are not necessarily restricted to intrinsic losses in the steel itself, but may also include losses due to flexing or friction in the clamps or the points of attachment at either the top or the bottom of the wire. The model only requires that the losses be associated with the motion of the wire in the region near the clamping through some angle θ from the vertical equilibrium position. This calculation assumes that for a given angle θ, there is some loss of energy $\Delta E(\theta)$ which is independent of the particular mode. The strategy therefore is to calculate the total energy of both the pendulum (E_p) and the violin (E_v) modes as a function of θ, and, by comparing $E_p(\theta)/\Delta E(\theta)$ with $E_v(\theta)/\Delta E(\theta)$, deduce the relationship between their Q's

The Pendulum

Simple physics gives the energy of the pendulum mode as a function of θ:

$$E_p(\theta) = Mgl(1 - \cos\theta)$$

M, g, and l are the mass, the acceleration due to gravity, and the length of the wire.

If we expand this result to second order in θ, we get

$$E_p(\theta) \approx Mgl\frac{\theta^2}{2}$$

The Violin Modes

If we approximate the wire to have no stiffness, which is valid for the parameters of the 40–meter prototype as far as the total energy of the lower order violin modes is concerned, then the potential energy of the violin mode is stored in the stretching of the wire. Therefore we can model the wire as a spring with spring constant k ($k = Y\sigma/l$; Y and σ are Young's Modulus and the cross sectional area). Consider the initial stretching when the mass is hung. The wire stretches to its equilibrium length, l, from its original length, l_o, according to

$$l = l_o + \Delta l$$

with

$$k\Delta l = Mg$$

Thus the energy is

$$E(\theta = 0) = \frac{1}{2}k(\Delta l)^2$$

Now consider the wire in the fundamental violin mode. The horizontal displacement of the wire, y, as a function of vertical position, z, at the maximum amplitude is

$$y(z) = y_o \sin\frac{\pi z}{l}$$

Then

$$\theta = \frac{dy}{dz}\bigg|_{z=o} = \frac{y_o\pi}{l}$$

The length, L, of the wire in the stretched position is

$$L = \int_o^l \sqrt{1 + (dy/dz)^2}\quad dz = \int_o^l \sqrt{1 + \theta^2\cos^2\left(\frac{\pi z}{l}\right)}\quad dz$$

$$\approx \int_o^l \left[1 + \frac{\theta^2}{2}\cos^2\left(\frac{\pi z}{l}\right)\right]dz = l + l\theta^2/4$$

The change in length ΔL from the zero energy length is

$$\Delta L = L - l_o = l - l_o + l\theta^2/4 = \Delta l + l\theta^2/4$$

And so the energy is

$$E_v(\theta) = \frac{1}{2}\,k(\Delta L)^2 = \frac{1}{2}k\left(\Delta l + l\theta^2/4\right)^2 \approx \frac{1}{2}k(\Delta l)^2 + \frac{1}{4}k\Delta l l\theta^2$$

Thus the potential energy of the violin mode is, accurate to second order in θ,

$$E_v(\theta) = E(\theta) - E(0) = \frac{1}{4}\,k\Delta l l\theta^2 = Mgl\theta^2/4$$

Generalization to 4 Wires

The pendulum has the same amount of energy at a given angle regardless of the number of wires. For a 4–wire system, however, each wire is only supporting one quarter of the mass, so the effective mass seen by the violin mode is M/4, and $E_v = Mgl\theta^2/16$. Therefore for a given angle θ, the pendulum mode has 8 times as much energy as a violin mode, $E_p = 8E_v$.

For the violin modes, the loss of energy per radian, ΔE_v, is given by

$$\Delta E_v(\theta) = E_v(\theta)/Q_v.$$

If the losses for both the violin mode and the pendulum mode are primarily in the bending of the wire, then the losses in the pendulum would equal the losses in the four wires:

$$\begin{aligned}\Delta E_p(\theta) &= \Delta E_{v1}(\theta) + \Delta E_{v2}(\theta) + \Delta E_{v3}(\theta) + \Delta E_{v4}(\theta) \\ &= \frac{E_p(\theta)}{8}\left(\frac{1}{Q_{v1}} + \frac{1}{Q_{v2}} + \frac{1}{Q_{v3}} + \frac{1}{Q_{v4}}\right)\end{aligned}$$

Therefore we can estimate the Q of the pendulum as

$$\frac{1}{Q_p} = \frac{1}{8}\left(\frac{1}{Q_{v1}} + \frac{1}{Q_{v2}} + \frac{1}{Q_{v3}} + \frac{1}{Q_{v4}}\right)$$

Appendix II: Thermal Lineshapes

The basis of our thermal lineshape comes from a paper by N. Mio[8] in which the mechanical transfer function of a pendulum with a finite mass wire is derived. His result is

$$\tilde{x}^2(f) = \frac{4k_BT}{\omega} \sum_{n=0}^{\infty} \frac{\omega_n^2/Q_n}{\mu_n \left[\left(\omega_n^2 - \omega^2\right)^2 + \omega_n^4/Q_n^2 \right]}$$

Here μ_n is the reduced mass of each mode, and is approximately equal to M for the pendulum mode (n=0) and $\frac{M}{2}\left(\frac{\omega_n}{\omega_p}\right)^2$ for the violin modes.

For a four-wire system the lineshape of an individual violin mode becomes

$$x_n^2(f) = \frac{2k_BT}{\omega} \frac{\omega_n^2/Q_n}{M(\omega_n/\omega_p)^2 \left[\left(\omega_n^2 - \omega^2\right)^2 + \omega_n^4/Q_n^2 \right]}$$

To get the appropriate factor of 2, realize that the mass the wire must push against is 4 times the mass giving the wire tension.

Then the thermal noise associated with one test mass is

$$\tilde{x}^2(f) = \frac{4k_BT}{\omega M} \frac{\omega_p^2/Q_p}{\left[\left(\omega_p^2 - \omega^2\right)^2 + \omega_p^4/Q_p^2 \right]} + \sum_{\text{4 wires}} \sum_{n=1}^{\sim 10^{20}} \tilde{x}_n^2(f)$$

To get the total thermal noise as in Figure 4, sum the contribution from all four test masses.

Notes

1. A. Gillespie, T. Lyons, and F. Raab, "Near Thermal Excitation of Violin Modes in the Test-Mass Suspension Wires of the 40–m Prototype Interferometer," 19 May 1992.
2. P. Saulson, *Phys. Rev. D*, **42**, 2437–2445 (1990).
3. In the case of the south end mass, which is normally used as the active element in the secondary cavity servo (i.e., the cavity is locked to the laser which is locked to the primary cavity), the ringdowns were measured with the south arm used alternately as either the primary or secondary cavity. The ringdowns were the same, indicating that the secondary servo did not damp the wire resonance. An order of magnitude estimate of the damping of the secondary servo puts a limit on the Q's as measured by a ringdown at roughly 10^6.
4. It was also verified that the pendulum damping piezos did not damp the wire resonances by measuring the ringdown with the piezos active, open circuit, and shorted. In each case the ringdown time was the same.
5. Steel music wire is used for all masses.
6. For a derivation, see Appendix II and reference 8.
7. This has been confirmed by S. Kawamura, Mark I Logbook 25, p. 74y.
8. N. Mio, *Jpn. J. Appl. Phys.*, **31**, 1243–1244 (1992).

Figure Captions

Figure 2

The data spectrum was taken with the electronic damping of the pendulum off; when the interferometer is in its normal operating configuration with the damping on, the wire resonances of this mass are excited above thermal noise by a factor of two. Next to two of the resonances are secondary peaks which are an order of magnitude smaller. These are presumably the transverse polarization mode of the violin resonances which are not efficiently coupled to the interferometer output. The large peak at 327.5 Hz is a calibration peak. The thermal noise lineshape has been averaged over each 0.025 Hz bandwidth to produce the prediction.

Figure 3

This spectrum is a blowup of the two central resonances in Figure 2 plotted on a linear scale to emphasize the peaks. The uncertainties of the data points are statistical errors due to eight averages in a power spectrum. (Because the frequency resolution is very fine, taking a spectrum requires a rather long time, and eight averages were the maximum number we were able to obtain before the interferometer fell out of lock.) The systematic uncertainty of the calibration is much smaller than these statistical errors.

Figure 4

The data were taken at two different bandwidths: 1.25 Hz from 200 to 1000 Hz and 6.25 Hz from 1000 to 2000 Hz. The thermal noise prediction was generated by integrating the lineshapes for each violin and pendulum mode over the appropriate bandwidth. The actual violin modes are much narrower than they appear on this plot and will look different depending on the bandwidth chosen. The data were taken with the electronic damping on, and the resonances around 320 Hz are excited a factor of two above thermal noise. The peaks in the noise spectrum between 1800 and 2000 Hz which roughly line up with the violin resonances are actually due to residual frequency noise from the laser (see for example Logbook #22).

Violin Resonance Q's

Left Arm

data of
7/23/92-
7/27/92

frequency (Hz)	Q
319.65	13,000
324.90	13,000
326.075	19,000
328.45	16,000

End Mass

594.35	242,000
596.675	335,000
598.15	43,000
605.025	112,000

Vertex Mass

Right Arm

592.7	295,000
592.8	295,000
596.425	356,000
600.225	163,000

Vertex Mass

505.85	66,000
506.875	118,000
512.85	23,000
514.90	16,000

End Mass

Figure 1.

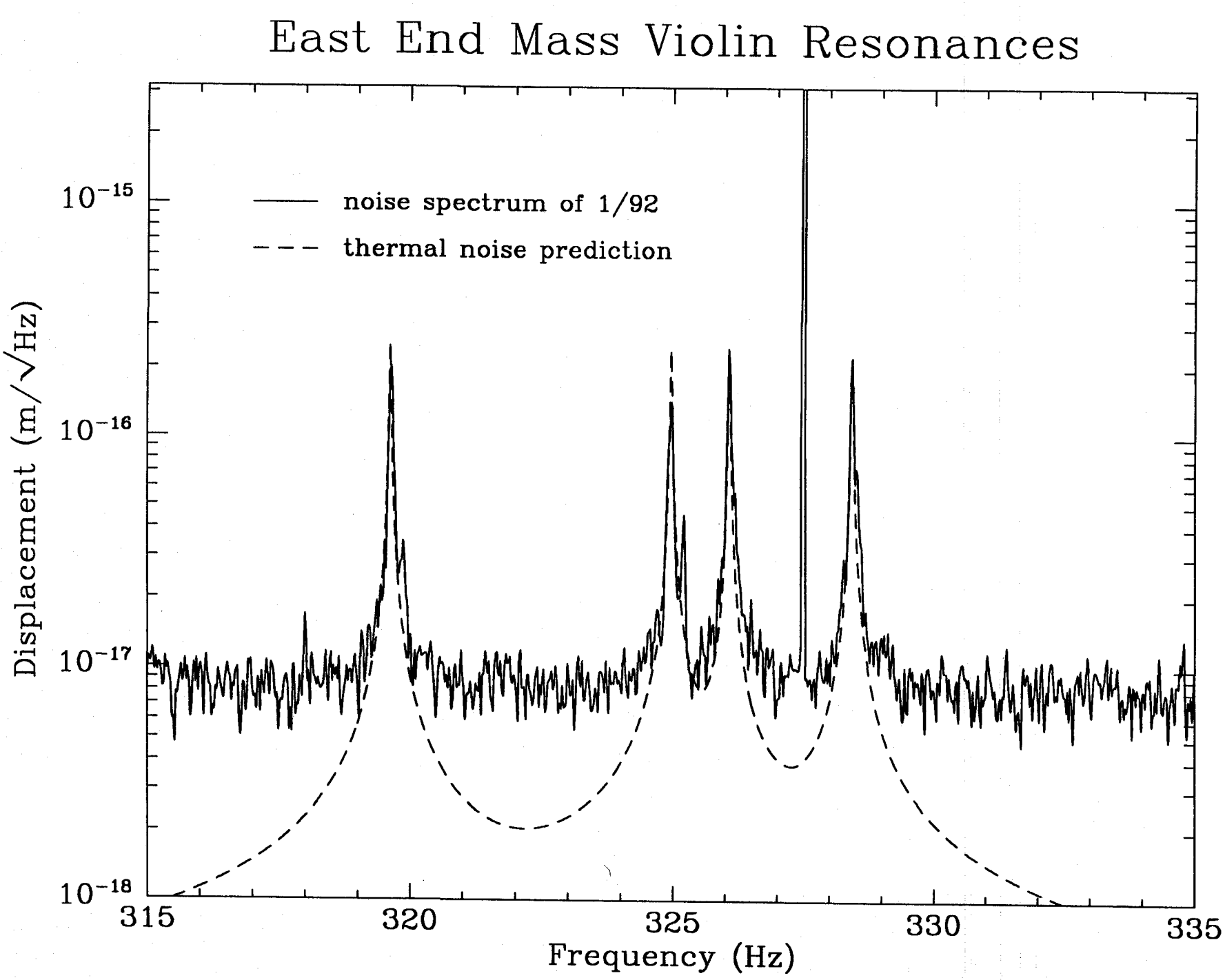
East End Mass Violin Resonances
noise spectrum of 1/92
thermal noise prediction
Displacement (m/√Hz)
10^-15
10^-16
10^-17
10^-18
315
320
325
330
335
Frequency (Hz)

Figure 2.

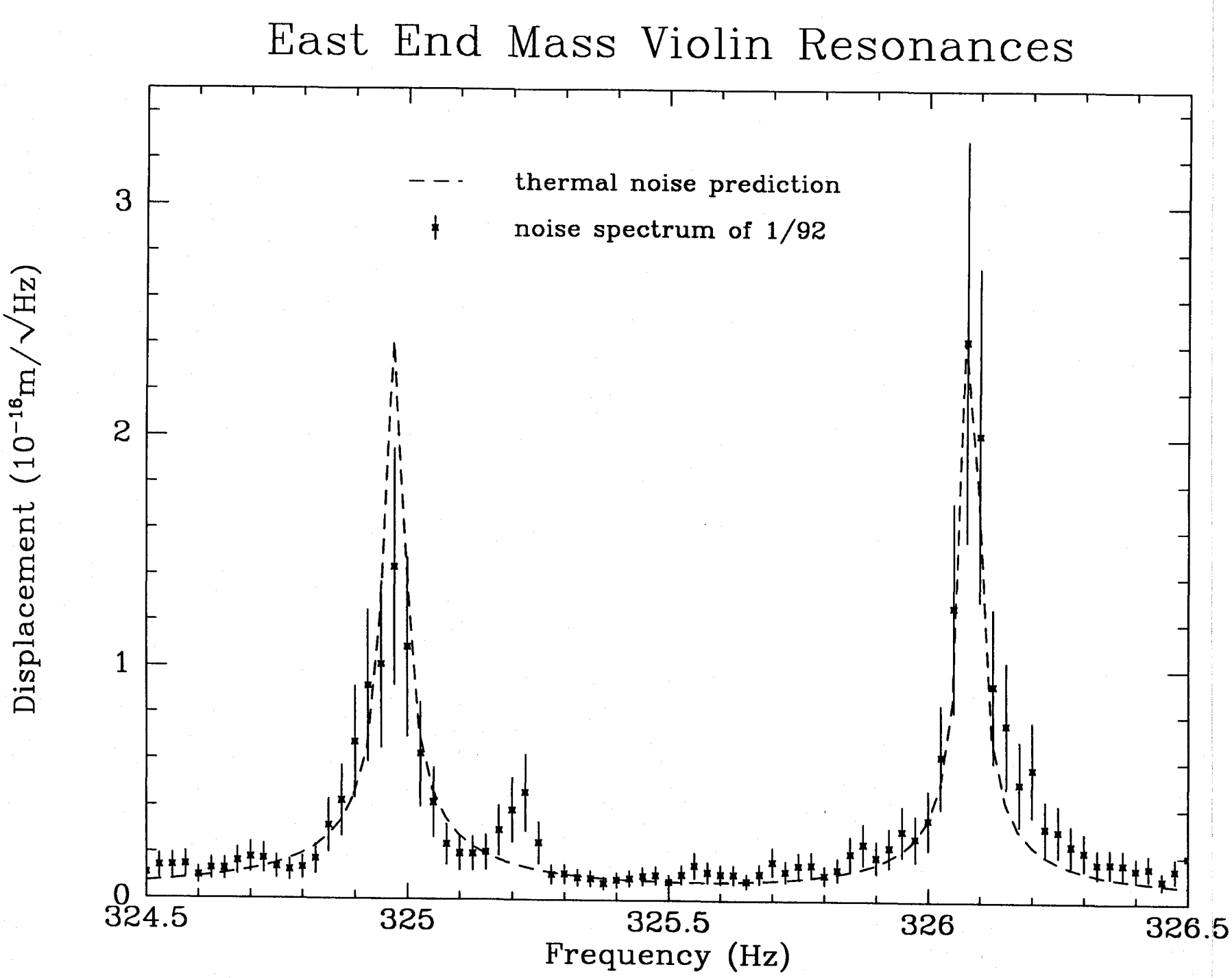
East End Mass Violin Resonances
thermal noise prediction
noise spectrum of 1/92
Displacement (10^{-16}m/$\sqrt{\text{Hz}}$)
0
1
2
3
324.5
325
325.5
326
326.5
Frequency (Hz)

Figure 1

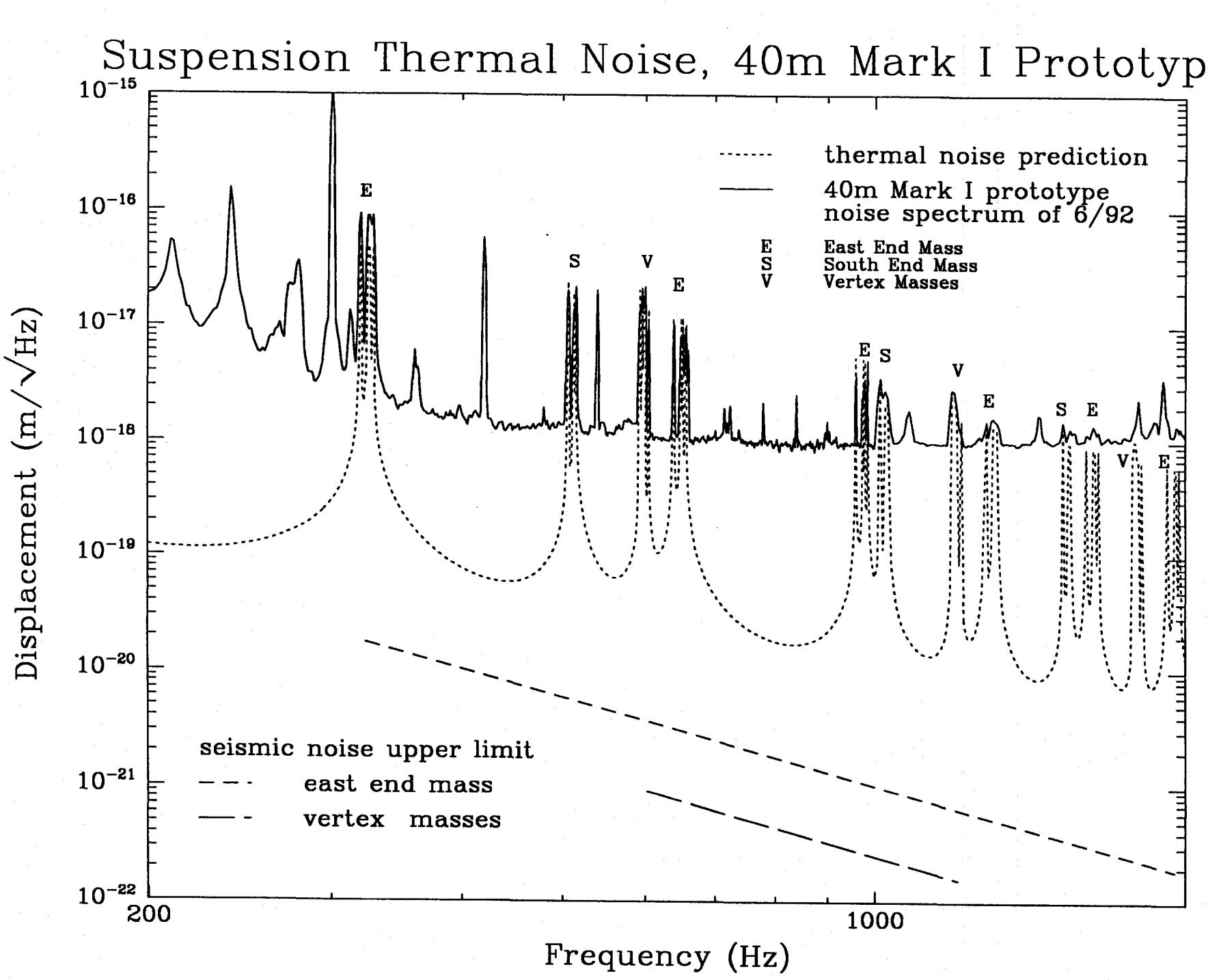
Suspension Thermal Noise, 40m Mark I Prototype
Displacement (m/√Hz)
Frequency (Hz)
thermal noise prediction
40m Mark I prototype noise spectrum of 6/92
E East End Mass
S South End Mass
V Vertex Masses
seismic noise upper limit
east end mass
vertex masses
10^-15
10^-16
10^-17
10^-18
10^-19
10^-20
10^-21
10^-22
200
1000

Figure 4.